

# Crystallographic and NMR Studies on Chiral Palladium(II) Allyl Ferrocene-Based P,N Complexes

Urs Burckhardt, Volker Gramlich, Patrick Hofmann, Reinhard Nesper,  
Paul S. Pregosin,\* Renzo Salzmänn, and Antonio Togni\*

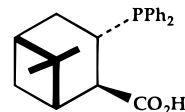
Laboratory of Inorganic Chemistry, Swiss Federal Institute of Technology, ETH Zentrum,  
8092 Zürich, Switzerland

Received February 27, 1996<sup>®</sup>

Detailed crystallographic and NMR measurements are reported for several Pd(II) allyl complexes containing chiral ferrocene-based phosphinopyrazole ligands, CpFe{ $\eta^5$ -C<sub>5</sub>H<sub>3</sub>(1-CH(CH<sub>3</sub>)(NN=C(R<sup>1</sup>CH=CR<sup>2</sup>)-2-PPh<sub>2</sub>))}, **1**. Relative to similar BINAP, CHIRAPHOS, and diphosphine JOSIPHOS analogs, the major isomer of the  $\beta$ -pinene allyl complex [Pd( $\eta^3$ -C<sub>10</sub>H<sub>15</sub>)(**1a**)]CF<sub>3</sub>SO<sub>3</sub>, **2**, R<sup>1</sup> = R<sup>2</sup> = H, shows a surprisingly large trans influence for the PPh<sub>2</sub> donor moiety, based on <sup>13</sup>C data. The solid-state structure for **2** shows normal bond lengths, although there are indications that the allyl adjusts its position due to the relatively large P,N ligand. The solid- and solution-state structures of [Pd( $\eta^3$ -PhCHCHCHPh)(**1g**)]PF<sub>6</sub>, **3g**, R<sup>1</sup> = adamantyl and R<sup>2</sup> = H (99% ee in the enantioselective allylic amination), show the allyl ligand to be strongly rotated, thus placing the terminal allyl carbon proximate to the pyrazole moiety, significantly below the coordination plane. These structural results suggest that, for the enantioselective catalysis using ligands **1**, there is an "early" transition state.

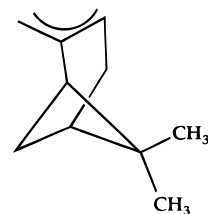
## Introduction

Stereoselective Pd-catalyzed reactions involving chelating ligands and  $\pi$ -allyl intermediates are of paramount importance. For the enantioselective allylic alkylation<sup>1</sup> one often finds ee's of the order of >90% using chelating diphosphines<sup>2–7</sup> or chelating diamines.<sup>8–10</sup> In recent studies it has been found that mixed donor combinations, e.g. P,N ligands,<sup>11,12</sup> can also be successfully employed, e.g. the chiral P,O ligand



often gives ee's of >95%.<sup>12c</sup>

In our studies on the structures and dynamics of complexes of the general type [Pd( $\pi$ -allyl ligand)(bidentate)](anion), using NOE and X-ray methods,<sup>13,14</sup> we have made extensive use of model complexes containing the  $\beta$ -pinene allyl ligand,  $\eta^3$ -C<sub>10</sub>H<sub>15</sub>:



$\beta$ -pinene allyl ligand,  $\eta^3$ -C<sub>10</sub>H<sub>15</sub>.

This allyl ligand is interesting in that it is of moderate size and can coordinate one face only. The structural data from these  $\beta$ -pinene allyl complexes with BINAP and other chiral ligands are informative in that they

- <sup>®</sup> Abstract published in *Advance ACS Abstracts*, July 1, 1996.
- (1) Togni, A.; Venanzi, L. M. *Angew. Chem., Int. Ed. Engl.* **1994**, *33*, 497. Hayashi, T. In *Catalytic Asymmetric Synthesis*; Ojima, I., Ed.; VCH Publishers: Weinheim, Germany, 1993; p 325. Reiser, O. *Angew. Chem.* **1993**, *105*, 576.
- (2) Mackenzie, P. B.; Whelan, J.; Bosnich, B. *J. Am. Chem. Soc.* **1985**, *107*, 2046. Auburn, P. R.; Mackenzie, P. B.; Bosnich, B. *J. Am. Chem. Soc.* **1985**, *107*, 2033.
- (3) Togni, A.; Breutel, C.; Schnyder, A.; Spindler, F.; Landert, H.; Tijani, A. *J. Am. Chem. Soc.* **1994**, *116*, 4062.
- (4) Hayashi, T.; Yamamoto, A. *Tetrahedron Lett.* **1988**, *29*, 669.
- (5) Sawamura, M.; Ito, Y. *J. Am. Chem. Soc.* **1992**, *114*, 2586.
- (6) (a) Trost, B. M.; van Vranken, D. L.; Bingel, C. *J. Am. Chem. Soc.* **1992**, *114*, 9327. (b) Trost, B. M.; Murphy, D. J. *Organometallics* **1985**, *4*, 1143.
- (7) Yamaguchi, M.; Shima, T.; Hida, M. *Tetrahedron Lett.* **1990**, *31*, 5049. Yamaguchi, M.; Shima, T.; Yamagishi, T.; Hida, M. *Tetrahedron: Asymmetry* **1991**, *2*, 663.
- (8) (a) von Matt, P.; Lloyd-Jones, G. C.; Minidis, A. B. E.; Pfaltz, A.; Macko, L.; Neuburger, M.; Zehnder, M.; Rügger, H.; Pregosin, P. S. *Helv. Chim. Acta* **1995**, *78*, 265. (b) Pfaltz, A. *Acc. Chem. Res.* **1993**, *26*, 339. (c) von Matt, P.; Pfaltz, A. *Angew. Chem., Int. Ed. Engl.* **1993**, *32*, 566. (d) Leutenegger, U.; Umbricht, C.; Fahrni, P.; von Matt, A.; Pfaltz, A. *Tetrahedron* **1992**, *48*, 2143. (e) Mueller, D.; Umbricht, B.; Weber, A.; Pfaltz, A. *Helv. Chim. Acta* **1991**, *74*, 232.
- (9) Togni, A. *Tetrahedron: Asymmetry* **1991**, *2*, 683. Bovens, M.; Togni, A.; Venanzi, L. M. *J. Organomet. Chem.* **1993**, *451*, C28.
- (10) (a) Tanner, D. *Angew. Chem., Int. Ed. Engl.* **1994**, *106*, 625. (b) Andersson, P. G.; Harden, A.; Tanner, D.; Norrby, P. O. *Chem. Eur. J.* **1995**, *1*, 12. Gamez, P.; Dunjic, B.; Fache, F.; Lemaire, M. *J. Chem. Soc., Chem. Commun.* **1994**, 1417.
- (11) Brown, J. M.; Hulmes, D. I.; Guiry, P. J. *Tetrahedron* **1994**, *50*, 4493.
- (12) (a) Sprinz, J.; Kiefer, M.; Helmchen, G.; Reggelein, M.; Huttner, G.; Zsolnai, L. *Tetrahedron Lett.* **1994**, *35*, 1523. (b) Sprinz, J.; Helmchen, G. *Tetrahedron Lett.* **1993**, 1769. (c) Knühl, G.; Sennhenn, P.; Helmchen, G. *J. Chem. Soc., Chem. Commun.* **1995**, 1845.

- (13) (a) Pregosin, P. S.; Rügger, H.; Salzmänn, R.; Albinati, A.; Lianza, F.; Kunz, R. W. *Organometallics* **1994**, *13*, 83. (b) Pregosin, P. S.; Rügger, H.; Salzmänn, R.; Albinati, A.; Lianza, F.; Kunz, R. W. *Organometallics* **1994**, *13*, 5040. (c) Ammann, C. J.; Pregosin, P. S.; Rügger, H.; Albinati, A.; Lianza, F.; Kunz, R. W. *J. Organomet. Chem.* **1992**, *423*, 415. (d) Rügger, H.; Kunz, R. W.; Ammann, C. J.; Pregosin, P. S. *Magn. Reson. Chem.* **1992**, *29*, 197. (e) Albinati, A.; Kunz, R. W.; Ammann, C.; Pregosin, P. S. *Organometallics* **1991**, *10*, 1800. (f) Albinati, A.; Kunz, R. W.; Ammann, C.; Pregosin, P. S. *Organometallics* **1990**, *9*, 1826. (g) Musco, A.; Pontellini, R.; Grassi, M.; Sironi, A.; Meille, S. V.; Rügger, H.; Ammann, C.; Pregosin, P. S. *Organometallics* **1988**, *7*, 2130.
- (14) (a) Pregosin, P. S.; Salzmänn, R.; Togni, A. *Organometallics* **1995**, *14*, 842. (b) Breutel, C.; Pregosin, P. S.; Salzmänn, R.; Togni, A. *J. Am. Chem. Soc.* **1994**, *116*, 4067. (c) Rügger, H.; Pregosin, P. S. *Magn. Reson. Chem.* **1994**, *32*, 297.

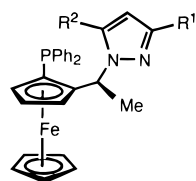
**Table 1. Selected Bond Lengths (Å)<sup>a</sup> and Angles (deg)<sup>a</sup> for **2** (Molecule A) and **3g****

<b>2</b> (molecule A)		<b>3g</b>	
Bond Distances			
Pd–P	2.317(3)	Pd–P	2.321(3)
Pd–N(1)	2.134(10)	Pd–N(2)	2.157(7)
Pd–C(1)	2.123(14)	Pd–C(35)	2.133(9)
Pd–C(2)	2.175(11)	Pd–C(34)	2.179(8)
Pd–C(3)	2.204(12)	Pd–C(33)	2.253(10)
C(1)–C(2)	1.39(2)	C(34)–C(35)	1.433(13)
C(2)–C(3)	1.42(2)	C(33)–C(34)	1.383(13)
N(1)–N(2)	1.36(2)	N(1)–N(2)	1.357(10)
Bond Angles			
N(1)–Pd–C(1)	164.4(5)	N(2)–Pd–C(35)	163.2(3)
P–Pd–C(1)	105.6(4)	P–Pd–C(35)	101.7(3)
C(1)–Pd–C(3)	68.4(6)	C(33)–Pd–C(34)	36.3(3)
P–Pd–N(1)	87.4(3)	P–Pd–N(2)	95.1(2)
P–Pd–C(3)	167.7(4)	P–Pd–C(33)	158.5(3)
N(1)–Pd–C(3)	97.2(5)	N(2)–Pd–C(33)	96.9(3)

<sup>a</sup>Numbers in parentheses are esd's in the least significant digits.

afford a comparison of these auxiliaries in terms of relative size (via X-ray and NOE studies) and donor properties (<sup>13</sup>C NMR of the allyl ligand).

In separate studies, we have shown that JOSIPHOS complexes are good catalysts for enantioselective allylic alkylation.<sup>3,15</sup> In general, the JOSIPHOS class is interesting since it is readily modified to afford a variety of chiral chelating P,P, P,N, or P,S ligands, many of which are excellent chiral auxiliaries.<sup>15c,d</sup> Specifically, the series of P,N ligands **1a–g** are excellent for the



<b>1</b>	R <sup>1</sup>	R <sup>2</sup>
<b>a</b>	H	H
<b>b</b>	CH <sub>3</sub>	CH <sub>3</sub>
<b>c</b>	CF <sub>3</sub>	CF <sub>3</sub>
<b>d</b>	Ph	CH <sub>3</sub>
<b>e</b>	9-anthryl	H
<b>f</b>	1-triptycyl	H
<b>g</b>	1-adamantyl	H

enantioselective allylic amination reaction with ee's routinely >95%.<sup>16</sup> The enantioselective allylic amination, in which a new C–N bond is formed, has received somewhat less attention<sup>17</sup> but is also readily accomplished with similar chiral auxiliaries.

We report here on two aspects of the Pd–allyl chemistry of **1**: (a) We extend our studies in which we compare solid-state and solution characteristics for [Pd(η<sup>3</sup>-C<sub>10</sub>H<sub>15</sub>)(**1a**)]CF<sub>3</sub>SO<sub>3</sub>, **2**, with related β-pinene allyl

(15) (a) Abbenhuis, H. C. L.; Burckhardt, U.; Gramlich, V.; Koellner, C.; Pregosin, P. S.; Salzmann, R.; Togni, A. *Organometallics* **1995**, *14*, 759. (b) Togni, A.; Breutel, C.; Soares, M.; Zanetti, N.; Gerfin, T.; Gramlich, V.; Spindler, F.; Rihis, G. *Inorg. Chim. Acta* **1994**, *222*, 213. (c) Abbenhuis, H. C. L.; Burckhardt, U.; Gramlich, V.; Togni, A.; Albinati, A.; Müller, B. *Organometallics* **1994**, *13*, 4481. (d) Togni, A.; Breutel, C.; Schnyder, A.; Spindler, F.; Landert, H.; Tijani, A. *J. Am. Chem. Soc.* **1994**, *116*, 4062. (e) Togni, A.; Häusel, R. *Synlett* **1990**, 633. (f) Burckhardt, U.; Hinterman, L.; Schnyder, A.; Togni, A. *Organometallics* **1995**, *14*, 5415.

(16) Togni, A.; Burckhardt, U.; Gramlich, V.; Pregosin, P.; Salzmann, R. *J. Am. Chem. Soc.* **1996**, *118*, 1031.

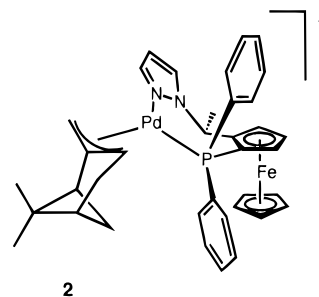
(17) Hayashi, T.; Yamamoto, A.; Ito, Y.; Nishioka, E.; Miura, H.; Yanagi, K. *J. Am. Chem. Soc.* **1989**, *111*, 6301.

complexes of CHIRAPHOS and BINAP. (b) We discuss structural properties of 1,3-diphenylallyl cationic Pd complexes of **1**, since this allyl is present in the palladium intermediate which arises from PhCH(OAc)–CH=CHPh as substrate.

## Results and Discussion

**β-Pinene Allyl Chemistry.** We start with a discussion of the solid-state and solution properties of the β-pinene allyl complex **2**. These data are interesting in that they help us to understand how the P,N-ligand **1a** interacts with a known allyl, relative to other chiral auxiliaries.

**X-ray Structure of [Pd(η<sup>3</sup>-C<sub>10</sub>H<sub>15</sub>)(**1a**)]CF<sub>3</sub>SO<sub>3</sub>.** The solid-state structure of the β-pinene allyl complex **2** was determined by X-ray diffraction methods. ORTEP



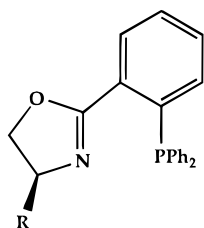
plots for the cation are shown in Figure 1. There are two independent molecules in the unit cell, and Table 1 shows a selected list of bond lengths and bond angles for molecule A (there are no significant differences in bonding parameters between the two molecules). Table 2 contains crystal and data collection parameters.

The coordination geometry about the Pd atom is distorted square planar with the terminal allyl carbon atoms, C(1) and C(3), and the P- and N-donor atoms of **1a** making up the immediate coordination sphere. The P atom is pseudo-trans to the allyl methine carbon, and the coordinated pyrazole N atom is pseudo-trans to the allyl methylene carbon.

There are several points worthy of note: (a) The methylene allyl carbon C(1) is ca. 0.30 Å and the methine allyl carbon C(3) is ca. 0.43 Å above the coordination plane defined by the Pd, P, and N atoms. Thus, the allyl is slightly rotated away from the PPh<sub>2</sub> moiety. A similar allyl rotation was observed for [Pd(η<sup>3</sup>-C<sub>10</sub>H<sub>15</sub>)(4,4'-dimethylbipyridine)](CF<sub>3</sub>SO<sub>3</sub>)<sup>13c</sup> suggesting that this slight distortion is a property of the β-pinene allyl ligand. (b) The plane of the three allyl carbons makes an angle of 126° with this same coordination plane (see Figure 1b). Although this angle is always >90° for allyl complexes,<sup>15,16</sup> 126° is slightly larger than those found previously in both the dimethylbipyridyl complex [Pd(η<sup>3</sup>-C<sub>10</sub>H<sub>15</sub>)(4,4'-dimethylbipyridine)](CF<sub>3</sub>SO<sub>3</sub>),<sup>15c</sup> 118°, and the BINAP derivative [Pd(η<sup>3</sup>-C<sub>10</sub>H<sub>15</sub>)(S-BINAP)]CF<sub>3</sub>SO<sub>3</sub>, 121°.<sup>13a,b</sup> Both P-phenyl ipso-carbons are on the same side of the coordination plane, with the pseudo-axial carbon ca. 1.44 Å and the pseudo-equatorial carbon ca. 0.23 Å from the plane. It is often the case for chelating diphosphine ligands that one ipso-carbon is above, and the other below, the coordination plane.<sup>17</sup> It is possible that this structural feature and the 126° angle reflect the relatively large size of this class of P,N ligand. The methyl group of the P,N-chelate ring lies approximately parallel to the upper Cp ring. In solution, a second conformation exists

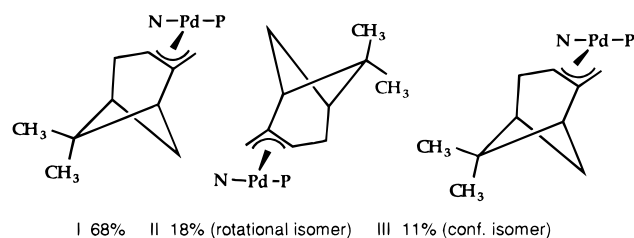
in which this methyl group is situated above this plane. Despite its relatively large size, ligand **1a** has a modest P–Pd–N bite angle of ca. 88°. This P–Pd–N angle can be as large as ca. 95°.<sup>16</sup>

The bond lengths and bond angles within the coordination spheres for both molecules are in agreement with the literature for Pd– $\pi$ -allyl complexes<sup>18,19</sup> with the Pd–C(1) distance of 2.123(14) Å, as expected, shorter than the Pd–C(3) bond length of 2.204(12) Å, due to the difference in trans-influence between nitrogen and phosphorus donors. Sprinz et al.<sup>12a</sup> have reported the solid-state structures for two Pd(II)  $\pi$ -allyl complexes of a chiral P,N-arylphosphino-oxazoline:



Interestingly, they find Pd–P and Pd–N separations of ca. 2.26 Å and ca. 2.09 Å, whereas our values are larger, ca. 2.32 and 2.14 Å, respectively; however, the observed Pd–P and Pd–N values for **2** are consistent with the corresponding Pd–P and Pd–N distances found<sup>16</sup> in (1,3-diphenylallyl)palladium complexes of **1d,f** as well as with the Pd–P separations observed in [Pd( $\eta^3$ -C<sub>10</sub>H<sub>15</sub>)(*R*(+)-BINAP)](CF<sub>3</sub>SO<sub>3</sub>), ca. 2.31–2.35 Å.<sup>13b</sup>

**NMR Studies on 2.** From <sup>1</sup>H and <sup>31</sup>P NMR spectroscopy, it is clear that **2** exists in at least three forms, I–III, in solution. From detailed <sup>1</sup>H-NOESY studies these can be assigned to the following (abbreviated) structures:



We note that there are strong NOEs in the major isomer from the pyrazole H(3) to both the allyl methine CH as well as to H<sup>d</sup> in keeping with the assigned structure of the major isomer and the expectation that substituents at this position of the pyrazole come forward toward the allyl ligand. This NOE, and those arising from the

(18) Regrettably, the relatively large experimental errors in the Pd–C bond lengths in this and other literature structures (e.g. ref 15b,c) make it unreasonable to discuss small, but perhaps chemically significant differences.

(19) (a) Smith, A. E. *Acta Crystallogr.* **1965**, *18*, 331. (b) Godleski, S. A.; Gundlach, K. B.; Ho, H. Y.; Keinen, E.; Frolow, F. *Organometallics* **1984**, *3*, 21. (c) Farrar, D. H.; Payne, N. C. *J. Am. Chem. Soc.* **1985**, *107*, 2054. (d) Murrall, N. W.; Welch, A. *J. Organomet. Chem.* **1986**, *301*, 109. (e) Facchin, G.; Bertani, R.; Calligaris, M.; Nardin, G.; Mari, M. *J. Chem. Soc., Dalton Trans.* **1987**, 1381. (f) Gozum, J. E.; Pollina, D. M.; Jensen, J.; Girolami, G. S. *J. Am. Chem. Soc.* **1988**, *110*, 2688. (g) Ozawa, F.; Son, T.; Ebina, S.; Osakada, K.; Yamamoto, A. *Organometallics* **1992**, *11*, 171. (h) Knierzinger, A.; Scholzer, P. *Helv. Chim. Acta* **1992**, *75*, 1211. (i) Ozawa, F.; Son, T.; Ebina, S.; Osakada, K.; Yamamoto, A. *Organometallics* **1992**, *11*, 171. (j) Yang, H.; Khan, A.; Nicholas, K. M. *Organometallics* **1993**, *12*, 3485. (k) Fernandez-Galan, R.; Manzano, B. R.; Otero, A.; Lanfranchi, M.; Pellingelli, A. *Inorg. Chem.* **1994**, *33*, 2309.

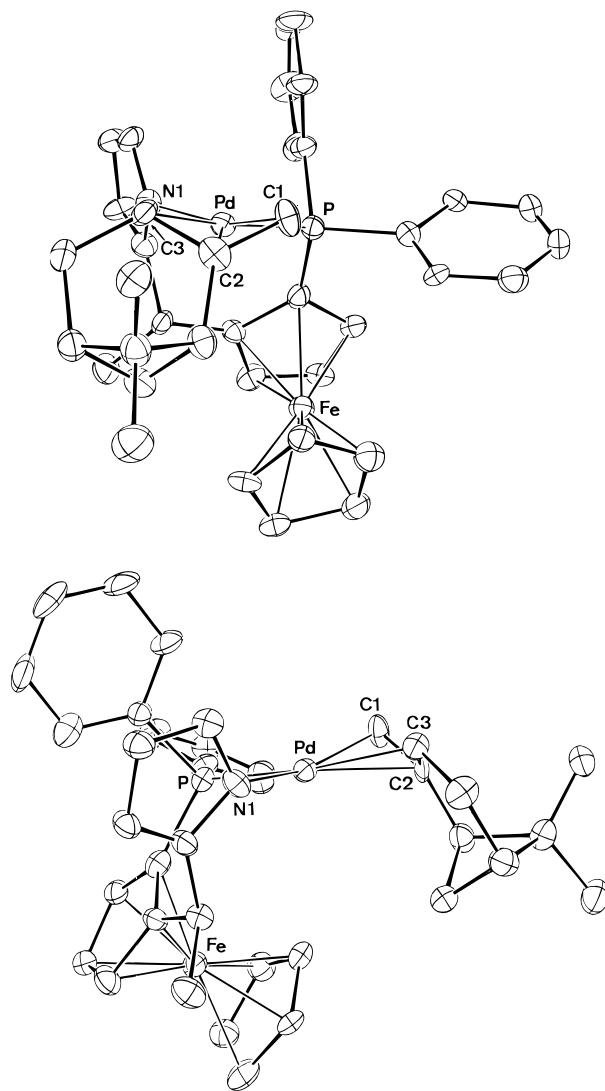
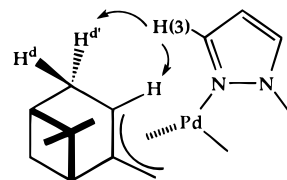


**Figure 1.** (a) Top: ORTEP view of **2** (molecule A) from behind the  $\beta$ -pinene allyl ligand looking toward **1a**. (b) Bottom: Side view of **2** showing that the allyl plane is directed away from the Pd atom and that the ferrocene moiety and the organic part of the allyl ligand are both on the same side of the coordination plane.



fragment of the structure showing NOEs from H(3)

ortho-protons of the P-phenyl groups, are critical for the assignments.

The major isomer I corresponds to the structure in the solid state. II is the rotational isomer of I, and III is a conformational isomer of I involving the chelate seven-membered ring, i.e.,

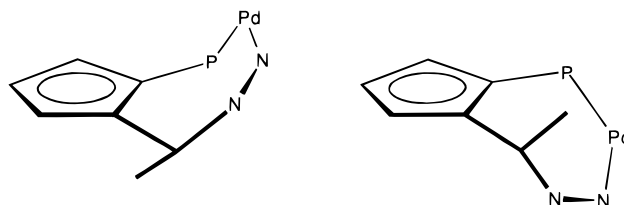


Table 2. Crystallographic Data for **2** and **3g**

	compd	
	<b>2</b>	<b>3g</b>
formula	C <sub>38</sub> H <sub>40</sub> PF <sub>6</sub> N <sub>2</sub> PdSO <sub>3</sub> F <sub>3</sub> ·0.25CHCl <sub>3</sub>	C <sub>52</sub> H <sub>52</sub> F <sub>6</sub> FeN <sub>2</sub> P <sub>2</sub> Pd
mol wt	855	1043.1
crystal dim, mm	0.3 × 0.3 × 0.5	0.3 × 0.3 × 0.4
color	red	red prism
data coll <i>T</i> (K)	140	293
cryst syst	monoclinic	orthorhombic
space group	<i>P2</i> <sub>1</sub>	<i>P2</i> <sub>1</sub> <i>2</i> <sub>1</sub> <i>2</i> <sub>1</sub>
<i>a</i> (Å)	10.992(3)	12.626(2)
<i>b</i> (Å)	10.551(2)	15.113(3)
<i>c</i> (Å)	33.833(10)	24.711(8)
$\beta$ (deg)	94.35(2)	
<i>V</i> (Å <sup>3</sup> )	3912.53	4715(2)
<i>Z</i>	4	4
$\rho$ (calcd) (g·cm <sup>-3</sup> )	1.502	1.469
abs coeff $\mu$ (mm <sup>-1</sup> )	1.028	0.819
<i>F</i> (000)	1802.0	2136
diffractometer	Scanner STOE IPDS	Syntex P21
radiation	Mo K $\alpha$ (graphite monochrom), $\lambda = 0.71073$ Å	
measd reflns	23 655	2543
index ranges	-13 ≤ <i>h</i> ≤ 13, -12 ≤ <i>k</i> ≤ 12, -41 ≤ <i>l</i> ≤ 41	0 ≤ <i>h</i> ≤ 12, 0 ≤ <i>k</i> ≤ 14, 0 ≤ <i>l</i> ≤ 23
2 $\theta$ range (deg)	8–52°	3–40°
no. of indep data coll	13 610 ( <i>R</i> (int) = 0.0588%)	2520 ( <i>R</i> (int) = 0.00%)
no. of obsd reflns ( <i>n</i> <sub>o</sub> )	12 847 ( <i>F</i> > 4.0 $\sigma$ ( <i>F</i> ))	2155 ( <i>F</i> > 4.0 $\sigma$ ( <i>F</i> ))
no. of params refined ( <i>n</i> <sub>r</sub> )	836	545
weighting scheme	$w^{-1} = \sigma^2(F_o^2) + (aP)^2 + bP$	$w^{-1} = \sigma^2(F) + 0.0010F^2$
<i>R</i> <sub>w</sub>	0.243 <sup>a</sup>	0.036
<i>R</i>	0.090 <sup>b</sup>	0.035
GOF	1.03	0.91

$$^a wR = (\sum w(F_o^2 - F_c^2)^2 / \sum w(F_o^2)^2)^{1/2}. \quad P = (F_o^2(\geq 0) + 2F_c^2)/3. \quad ^b R = \sum ||F_o| - |F_c|| / \sum |F_o|.$$

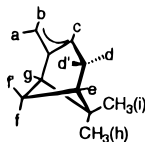
Table 3. Selected NMR Data for **2**

	I	II	III	IV <sup>a</sup>
Distribution	68%	18%	11%	3%
$\delta^{31P}$	14.8	13.1	17.0	12.3

	I		II		III	
	$\delta^1H$	$\delta^{13}C$	$\delta^1H$	$\delta^{13}C$	$\delta^1H$	$\delta^{13}C$
a	3.85	55.7	4.34	78.9	2.99	55.6
b	2.90	55.7	4.39	78.9	2.27	55.6
c	4.79	91.1	4.67	63.8	4.56	89.8
d'	1.91	30.4	1.54	30.2	2.19	29.0
e	2.20	39.3	1.90	39.4	2.39	39.3
f'	1.59	33.2	0.94	32.2	1.79	33.3
g	2.57	46.0	2.28	46.5	2.29	46.3
cp	3.89	70.9	3.91	71.2	3.33	70.3
CHCH <sub>3</sub>	2.10	18.3	2.16	18.2	2.33	25.1
CHCH <sub>3</sub>	6.05	57.8	6.55	57.2	5.96	57.7

<sup>a</sup> Isomer IV not identified, CDCl<sub>3</sub>, 253 K. Key:



In conformation III the methyl group on the stereogenic carbon lies above the upper Cp ring and thus shows an NOE to the ortho protons of the "upper" P-phenyl ring. There is a fourth complex, at about the 3% level, which we have not identified. Selected NMR data are given in Table 3.

The <sup>13</sup>C chemical shifts for the terminal allyl carbons in the major isomer of **2**,  $\delta = 55.7$  and  $\delta = 91.1$  for the

CH<sub>2</sub> and CH signals, respectively, are somewhat surprising. For the analogous<sup>13b,d,f</sup>  $\beta$ -pinene Pd(II) complexes with BINAP, CHIRAPHOS, a diphosphine JOSIPHOS, phenanthroline, and bipyridine, one finds<sup>13a</sup> the ranges 60.0–74.7 ppm (CH<sub>2</sub>) and 67.5–86.4 ppm (CH) for these two <sup>13</sup>C signals. Consequently, these <sup>13</sup>C values for **2** represent both new low- and new high-frequency extremes for the  $\eta^3$ -C<sub>10</sub>H<sub>15</sub> ligand in a cationic Pd compound. This may be a hint with regard to unexpected electronic properties of this P,N ligand; i.e., the P and N donors in **2** are exercising unexpectedly large and small trans influences, respectively. This is important to keep in mind, since, in the catalytic amination, the amine is known to attack at the allyl carbon trans to the P donor exclusively.<sup>16</sup> Unfortunately, we see no clear confirmation of these effects in the solid state,<sup>18</sup> although the terminal Pd–C(allyl) separations show the expected trend.

Analysis of the phase-sensitive NOESY cross-peaks shows that isomers I and III in **2** are in equilibrium; i.e., the chelate ring flips readily from one conformation to the other at ambient temperature. However, I and II, the allyl rotational isomers, are not exchanging under these conditions. This selectivity in the exchange is readily seen from the <sup>31</sup>P 2-D exchange spectrum, shown in Figure 2.

The proton resonances at ambient temperature were broad, so that the detailed assignment was made at 253 K, and a summary of these <sup>1</sup>H NMR data is also provided in Table 3. The equilibrium between I and III is interesting since a rigid conformation is thought to be a useful prerequisite for a successful auxiliary.

We conclude from the solution data that the <sup>13</sup>C  $\beta$ -pinene terminal allyl chemical shifts are somewhat extreme in nature, relative to conventional chelating phosphines and bipyridine type ligands. Coordinated **1a** can be expected to demonstrate some conformational

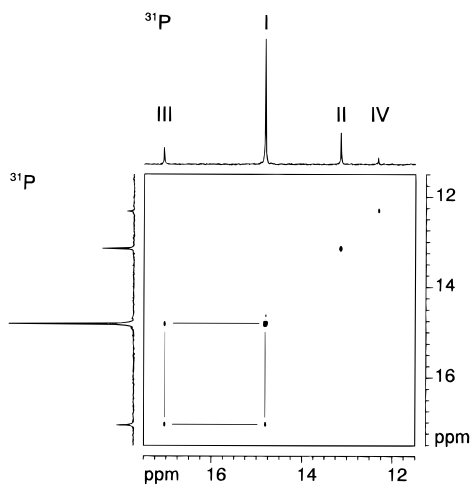
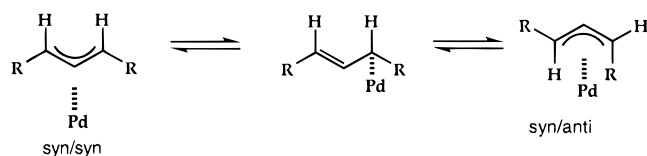


**Figure 2.** 2-D  $^{31}\text{P}$  exchange spectrum showing that the two  $^{31}\text{P}$  resonances arising from I and III (ring conformational isomers) are in equilibrium (THF- $d_6$ , 200 MHz).

lability, but the most stable isomer is that found in the solid state.

**1,3-Diphenylallyl Complexes.** As there are  $\eta^3$ -1,3-diphenylallyl cationic intermediates in the enantioselective allylic amination using ferrocene-based P,N ligands,<sup>16</sup> we have made additional solution studies on the complexes  $[\text{Pd}(\eta^3\text{-PhCHCHPh})(\mathbf{1b-g})]\text{PF}_6$ , **3b-g**. Given the conformational equilibria described above for **2** and the possibility for both syn/syn and syn/anti  $\eta^3$ -diphenylallyl geometric isomers,<sup>13a,20-23</sup> i.e.,



it is not surprising that we find up to four species in solution for **3b-f**, although these differ in abundance and structure as a function of **1**. Interestingly, **3g** exists almost exclusively in one form. In Chart 1 we show the populations and indicate the equilibria, observed via 2-D exchange spectroscopy, for these cationic species. The populations were obtained at 313 K, the temperature employed in the allylic amination reaction, but the NMR assignments were made using spectra recorded at ambient temperature. The relative amounts are important in that, if one assumes that the amine nucleophile attacks trans to the P-donor and at about the same rate for all isomers, then these populations do not always correlate with the observed enantiomeric excesses.<sup>16</sup> Consequently, these diastereoisomers react with the nucleophile at different rates as suggested earlier.<sup>22</sup>

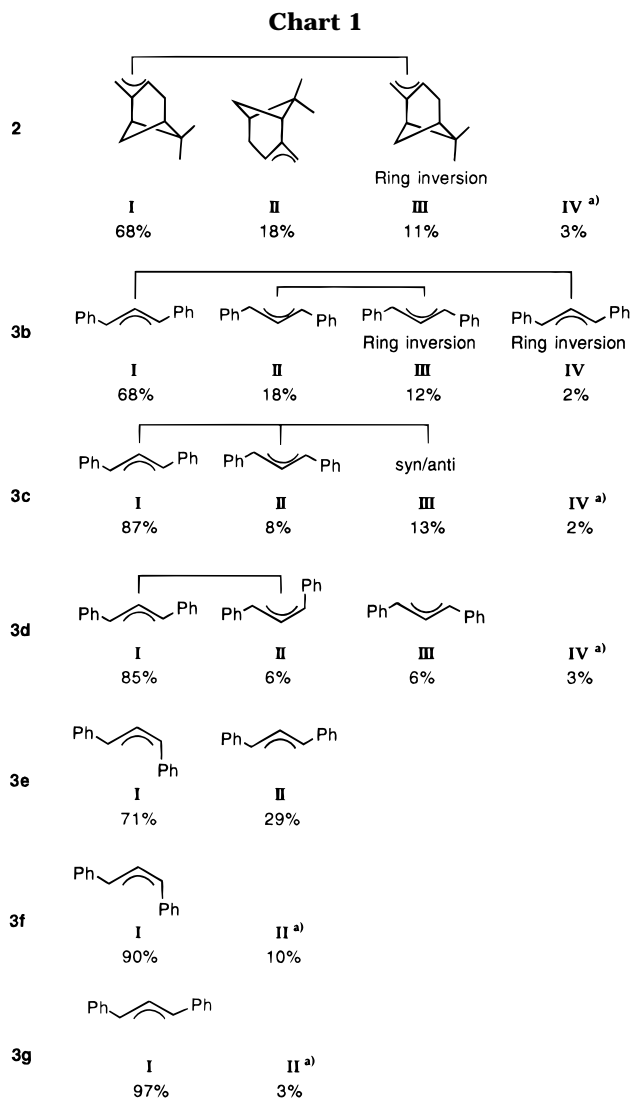
In connection with **3b-g**, there are several interesting details worth noting: (a) There is an empirical dependence of the  $^{31}\text{P}$  chemical shift on the chelate ring conformation with the minor conformer (methyl group

(20) Pregosin, P. S.; Salzman, R. *Magn. Reson. Chem.* **1994**, *32*, 128.

(21) Herrmann, J.; Pregosin, P. S.; Salzman, R.; Albinati, A. *Organometallics* **1995**, *14*, 3311 (dynamics and structure of PhCHCHPh allyl and  $\text{C}_3\text{H}_5$  allyl complexes of a new chiral P,S ligand).

(22) Barbaro, P.; Pregosin, P. S.; Salzman, R.; Albinati, A.; Kunz, R. *Organometallics* **1995**, *14*, 5160 (dynamics and catalysis of chiral BIPHEMP and 1,2-(diphenylphosphino)cyclopentane allyl complexes, among others).

(23) Gogoll, A.; Ornebro, J.; Grennberg, H.; Bäckvall, J. E. *J. Am. Chem. Soc.* **1994**, *116*, 3631.

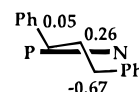


a) Structure not assigned.

above the Cp plane) often 8–9 ppm to high frequency of the major conformer (methyl group ca. parallel to the Cp plane) and (b) there is almost always<sup>14a,b,15a,16,22</sup> selectivity in the exchange processes between the various isomers; however for the 3,5-bis(trifluoromethyl) complex, **3c**, the three major diastereoisomers are all in equilibrium, as shown in Figure 3.

**X-ray Structure of 3g.** The structure of **3g** (ligand with (*S*)-(*R*) configuration) was determined by X-ray diffraction methods, and an ORTEP plot of the cation is shown in Figure 4. A selection of bond lengths and angles and crystallographic data are given in Tables 1 and 2, respectively. The coordination geometry about the Pd atom can be estimated to be severely distorted square planar with the allyl carbon atoms, C(33), C(34), and C(35), and the P- and N-donor atoms of **1g** making up the immediate coordination sphere.

The structure of **3g** reveals two unique aspects: There is a major displacement of the allyl group with respect to the P–Pd–N coordination plane (indicated as the bold line), and the relative position, in Å, of each of the three allyl carbons is shown as



These distances reflect a ca. 20° clockwise rotation of

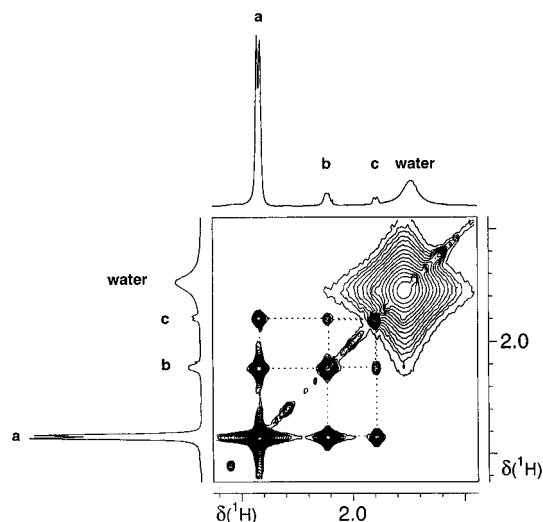


**Figure 3.** 2-D  $^1\text{H}$  exchange spectrum showing the three methyl  $^1\text{H}$  resonances arising from I–III (exo/endo plus one syn/anti) in **3c** which are all in equilibrium (THF- $d_6$ , 500 MHz).

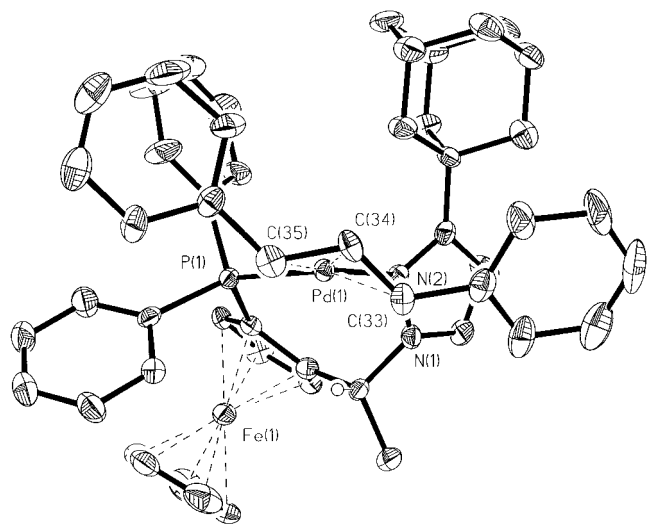


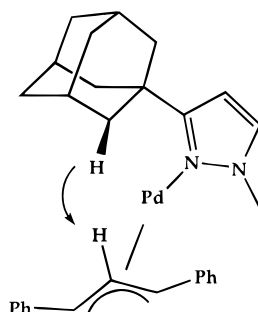
**Figure 4.** ORTEP view of the cation **3g**.

the allyl ligand with the terminal allyl carbon pseudo-trans to phosphorus well below the coordination plane and away from the pyrazole. The angle between the coordination plane and the plane defined by the three allyl carbons is  $132.3^\circ$ . Angles of ca.  $110$ – $115^\circ$  are often found in palladium allyl complexes. In Pd(II) complexes with large chiral auxiliaries, this angle is typically ca.  $120$ – $125^\circ$ . In the phosphino–oxazoline 1,3-diphenylallyl analog of Sprinz et al.<sup>12a</sup> this angle is  $110^\circ$ , for the P,N complex **2**, above, the value is  $126^\circ$ , and, in the 1,3-diphenyl allyl analog, **3d**, reported earlier, this angle is  $122.6^\circ$ . The observed value of  $132.6^\circ$  in **3g** represents the largest such interplanar angle found for an allyl complex and is certainly the result of the presence of the bulky adamantyl substituent. As mentioned in the discussion for **2**, these points represent “soft” energetic alternatives for an allyl ligand; however, these are both somewhat exaggerated in **3g**.

Additionally, we note that the allyl phenyl proximate to the  $\text{PPh}_2$  moiety is placed *between* the two P-phenyl groups, a point to which we shall return, and that the allyl phenyl near to the pyrazole donor is placed in the open space below the pyrazole moiety. Further, the P atom is ca.  $0.3 \text{ \AA}$  above the plane of the Cp to which it is attached.

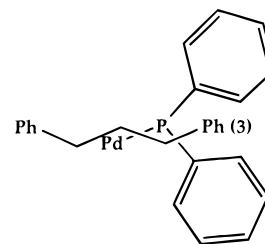
The various bond lengths and angles within the coordination sphere are within the expected limits. The P–Pd–N angle of  $95.1(2)^\circ$  is larger than that found in **2** but similar to the  $95.0(3)^\circ$  value found in **3d**. The Pd–P and Pd–N distances,  $2.321(3)$  and  $2.157(7) \text{ \AA}$ , respectively, are normal; however, the Pd–N separation is on the longish side. The distances to the two terminal allyl carbon atoms also reflect the differing trans influences of the P- and N-donors,  $2.253(10)$  and  $2.133(9) \text{ \AA}$ , respectively. Consequently, despite the substantial rotation, there is no marked lengthening of the Pd–C(allyl) separations. The C–C bond lengths within the allyl ligand are noteworthy:  $1.433(13) \text{ \AA}$  for C(34)–C(35) and  $1.383(13) \text{ \AA}$  for C(33)–C(34), suggesting somewhat more double-bond character between C(33) and C(34), again, in keeping with the donor properties of the P- and N-ligand types, respectively.

**Solution Structure of 3g.** Since the 3-adamantyl complex, **3g**, affords the largest ee in the allylic amination, ca. 99%,<sup>16</sup> we have also investigated its solution NMR characteristics. There is essentially only one component in solution (>97%), although there is evidence for a small quantity of a second component which is in slow exchange with the major isomer, as shown by exchange spectroscopy. The structure of the major isomer is readily defined via various NOEs, e.g.



Structural fragment showing NOE from allyl central proton to an adamantyl proton.

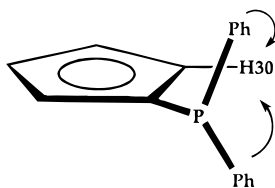
This Overhauser effect demonstrates the *exo* orientation of the allyl (the rotational isomer called *exo* has the central allyl C–H directed away from the  $\eta^5\text{-Cp}$ , whereas the *endo* isomer has the central allyl C–H directed toward the  $\eta^5\text{-Cp}$ ).<sup>16</sup> Further, there are two modest NOEs from the *ortho* protons of allyl phenyl(3), *cis* to the  $\text{PPh}_2$  moiety, to the **two** sets of proximate *ortho* protons from the P-phenyl groups (see Figure 5). This suggests that the allyl phenyl(3) lies in the space between these, i.e.



fragment showing the relative placement of Ph(3)

The relative placement of the two P-phenyl groups, with respect to the “upper” Cp ring is determined by the observation of two almost identical, strong NOEs from these same *ortho* protons of the P-phenyl groups

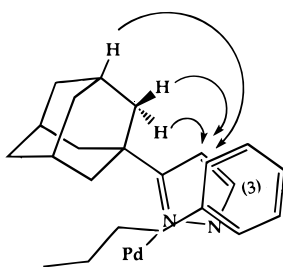
to the "upper" Cp-proton H(30), which is immediately adjacent to the P–C(Cp) bond, i.e.,



fragment showing the source of the two strong NOEs to H(30).

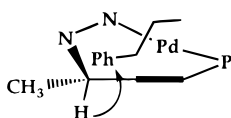
These NOE's concerning the ortho protons of the P-phenyls and H(30) are also shown in Figure 5.

There are *four* interesting NOE's which strongly suggest allyl rotation. Three of these, shown in Figure 6, arise from contacts between the ortho allyl phenyl(3) protons and three different adamantyl protons as shown:



NOE's from the three adamantyl protons to the ortho protons of allyl phenyl(3).

These develop due to the counterclockwise allyl rotation ((*R*)-(*S*) ligand configuration). The fourth stems from the interaction between the ortho allyl phenyl(1) protons and the chiral carbon methine proton CHCH<sub>3</sub>.



fragment showing NOE from methine CH of chiral carbon to ortho allyl phenyl (1) protons. This is only realistic if the allyl is strongly rotated.

It is fair to say that the qualitative NOE results would not have predicted the extent of the rotation. Finally, we note that, since we find only four adamantyl-<sup>13</sup>C signals, there is no restricted rotation of this substituent.

Given the <sup>13</sup>C data for the β-pinene allyl complex **2**, one wonders whether the same P,N-ligand electronic effect is operating in the 1,3-diphenylallyl complexes. Table 4 shows the terminal allyl <sup>13</sup>C chemical shifts for **3g** ( $\delta(^{13}\text{C}) = 107.9$  and  $65.9$ ) together with those for several model complexes, e.g., with BINAP and, more importantly, QUINAP, the chiral P,N ligand reported

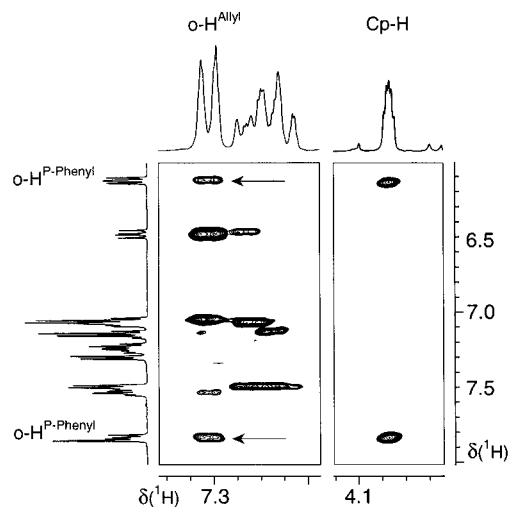
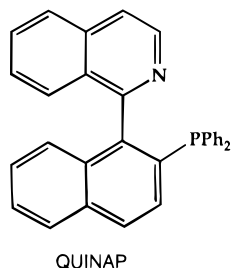


**Figure 5.** Two separate sections of the <sup>1</sup>H 2-D NOESY of **3g** showing the NOE's from the two ortho P-phenyl protons to (left) the ortho protons of the allyl phenyl(3) and (right) the Cp proton H(30). The "upper" ortho P-phenyl protons resonate at lowest frequency (500 MHz, THF-*d*<sub>8</sub>).

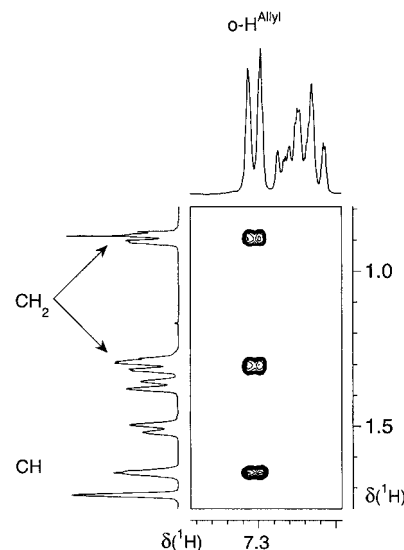


**Figure 6.** Section of the <sup>1</sup>H 2-D NOESY of **3g** showing the NOE's deriving from the interaction between the ortho protons of the allyl phenyl(3), which is proximate to the PPh<sub>2</sub> group, to three different adamantyl protons. These are feasible only if the allyl ligand is rotated (500 MHz, THF-*d*<sub>8</sub>).

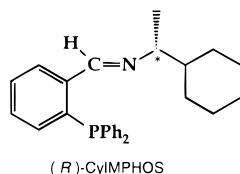
**Table 4. Terminal Allyl <sup>13</sup>C Chemical Shifts for Selected 1,3-Diphenylallyl Complexes [Pd( $\eta^3$ -PhCHCHCHPh)(chelate)]<sup>+</sup>**

chelate	$\delta(^{13}\text{C})$	chelate	$\delta(^{13}\text{C})$
<b>1g</b>	107.9, <sup>a</sup> 65.9 <sup>b</sup>	<i>S</i> -BINAP <sup>e</sup>	104.6, 87.2
<i>S</i> -QUINAP <sup>c</sup>	98.4, <sup>a</sup> 72.9 <sup>b</sup>	<i>S,S</i> -CHIRAPHOS <sup>e</sup>	90.1, 88.1
( <i>R</i> )-CyIMPPOS <sup>e</sup>	104.5, 67.9	dppe <sup>e</sup>	91.7
<i>R,S</i> -JOSIPHOS <sup>d</sup>	96.4, 82.0	bipy <sup>e</sup>	78.9

<sup>a</sup> Trans to P. <sup>b</sup> Trans to N. <sup>c</sup> From ref 11. <sup>d</sup> (*R,S*)-JOSIPHOS = (Cp)Fe{C<sub>5</sub>H<sub>3</sub>(1-CH(CH<sub>3</sub>)PCy<sub>2</sub>)-2-PPh<sub>2</sub>}; see ref 14. <sup>e</sup> Data from ref 22.

by Brown and co-workers.<sup>11</sup> Again the observed terminal allyl chemical shifts for the P,N ligand, in this case, ligand **1g** in complex **3g**, afford extreme high- and low-frequency signals for the allyl carbons trans to P and trans to N, respectively. We have previously reported details for **3d**,<sup>16</sup> including its X-ray structure: Pd–P = 2.321(4) Å, Pd–N = 2.131(11) Å,  $\delta(^{13}\text{C}) = 104.4$  (trans

to P) and 67.9 (trans to N), ee = 96%. The distances are not exceptional; however, once again, the two terminal allyl  $^{13}\text{C}$  chemical shifts are relatively extreme, if not quite as pronounced as in **3g**. We do not suggest that these chemical shifts in any way directly reflect on the effectiveness of the ligand as an auxiliary in the enantioselective catalytic reaction; indeed, for  $[\text{Pd}(\eta^3\text{-PhCHCHCHPh})(R)\text{-CyIMPPOS}]^+$ , one observes a low



ee<sup>22</sup> but the complex has terminal  $^{13}\text{C}$  allyl chemical shifts very close to those of **3d**. Nevertheless, these NMR results are interesting in themselves and reflect useful ground-state properties of such chelating P,N ligands in that they significantly differentiate between the two allyl termini.

**Comments and Conclusions.** The solid- and solution-state structures of **3g** show the allyl ligand to be strongly rotated, thus placing the terminal allyl carbon proximate to the pyrazole moiety, significantly below the coordination plane. The result of this rotation is a ground-state structure in **3g** (and **3d**) which resembles a potential Pd(0) transition-state structure. These structural results suggest that, for the enantioselective catalysis using ligands **1**, one is dealing with an "early" transition state. It has been suggested,<sup>10b</sup> on the basis of calculations, that such a rotated ground-state structure might be an important mechanistic feature of the enantioselective allylic alkylation.

Equally interesting (and important, as this determines the enantiomer produced) is that we observe the exo isomer and not the endo isomer. An undistorted exo-allyl complex would have the allyl phenyl(1) closer to the adamantyl moiety than would the corresponding endo derivative. Complex **3g** circumvents part of the problem by an allyl rotation; however, this alone is not sufficient. A simple rotation would result in placement of the remaining allyl phenyl(3) in an unfavorable stacking position relative to a proximate P-phenyl. However, by strongly bending the allyl plane away from the chiral ligand, one can conveniently slot the allyl phenyl(3) between the two P-phenyl groups, thus obtaining an optimal steric placement on both sides.

Summarizing, ligand **1g** makes use of the trans influence difference (P-donor > N-donor) to steer the nucleophile toward one side of the allyl and subtle steric effects to select the correct allyl isomer. In general, the  $\eta^3$ -1,3-diphenylallyl complexes, **3**, exist in solution as a series of allyl rotational, chelate-ring conformational, and/or allyl geometric isomers. The terminal allyl  $^{13}\text{C}$  shifts bestowed by this type of P,N ligand are fairly extreme.

## Experimental Section

**X-ray Crystallographic Studies.** Table 2 provides experimental and crystallographic data concerning compounds

**2** and **3g**. Intensity data for complex **2** were collected at a temperature of 140 K on a STOE IPDS (image plate detector system). The program EXPOSE<sup>24</sup> was used for the data collection. The unit cell dimensions were obtained by the applying the program CELL.<sup>24</sup> Finally the data reduction was performed using CONVERT.<sup>24</sup> The structure was solved with the program SHELXS-86<sup>25</sup> and refined with SHELXL-93.<sup>26</sup> Molecular graphics were performed by ORTEP II.<sup>27</sup> Least-squares methods with anisotropic thermal parameters for all non-hydrogen atoms were used in the refinement of both compounds. All hydrogen atom positions were placed in calculated positions with fixed isotropic parameters ( $U_{\text{iso}} = 0.080 \text{ \AA}^2$ ). For **2**, some slightly disordered parts of the compound were refined with constraints or restraints. The C–F distance was fixed to 1.320(1) Å, and the anisotropic thermal parameters were set to be equal for the three fluorine atoms in their respective molecules. The same thermal constraint was applied to the three chlorine atoms in the solvent molecule.

**NMR Spectroscopy.** The NMR spectra were recorded at room temperature on a Bruker AMX 500 instrument operating at 500.1 MHz for  $^1\text{H}$  and 125.8 MHz for  $^{13}\text{C}$ . Chemical shifts are given in ppm relative to TMS and external 85%  $\text{H}_3\text{PO}_4$ . The FID's were treated with an exponential factor (3 Hz line broadening) for  $^{31}\text{P}$  and  $^{13}\text{C}$  to obtain the final 1-D data set. In some cases resolution enhancement was used to resolve partially overlapping lines.  $^{13}\text{C}$  assignments were made with the help of literature values plus DEPT and 2-D correlation measurements. NOESY spectra were recorded using a 0.8 s mixing time.

**Synthesis.** Complex **2**, as a pale yellow solid, was prepared in 71% yield by starting from the chloro-bridged dinuclear pinene allyl complex by the addition of  $\text{AgCF}_3\text{SO}_3$  and **1a** in MeOH. We have described this simple type of synthesis previously. Suitable crystals could be obtained from  $\text{CHCl}_3/\text{ether}$ . Calcd for  $\text{C}_{38}\text{H}_{40}\text{F}_3\text{FeN}_2\text{O}_3\text{P}_2\text{PdS}$  (MW = 885.6): C, 51.51; H, 4.55; N, 3.16. Found: C, 51.29; H, 4.67; N, 3.43. The ligands **1** and the complexes **3** have been reported previously.<sup>15f,16</sup>

**Acknowledgment.** U.B. thanks Lonza Ltd. for financial support; P.S.P. thanks the Swiss National Science Foundation as well as the ETH for support and the Johnson-Matthey Research Foundation, Reading, England, for the loan of precious metals. We also thank Dr. H. Rügger for helpful discussion and experimental support and Prof. C. Bianchini for (R)-CyIMPPOS.

**Supporting Information Available:** Tables of complete atomic coordinates and  $U$  values, anisotropic displacement parameters, complete interatomic distances and bond angles, and data collection parameters for compounds **2** and **3g** and ORTEP views of **3g** and of the two crystallographically independent molecules of **2** showing complete atom numbering schemes (29 pages). Ordering information is given on any current masthead page. Tables of calculated and observed structure factors for both compounds may be obtained from the authors upon request.

OM960130+

(24) Stoe & Cie Scanner Stoe IPDS diffractometer software, version 1.08; Stoe & Cie, Darmstadt, Germany, 1993.

(25) Sheldrick, G. M. SHELXS-86. Program for the Solution of Crystal Structures, University of Göttingen, Germany, 1985.

(26) Sheldrick, G. M. SHELXS-93. Program for the Refinement of Crystal Structures, University of Göttingen, Germany, 1993.

(27) Larson, A. C.; Lee, F. L.; Le Page, Y.; Webster, M.; Charland, J. P.; Gabe, E. J. NRCVAX Crystal Structure System with interactive version of ORTEP II, NRC, Ottawa, Canada, 1986.